

# Benthic Microbial Fuel Cell as Direct Power Source for an Acoustic Modem and Seawater Oxygen/Temperature Sensor System

Yanming Gong,<sup>†</sup> Sage E. Radachowsky,<sup>†,§</sup> Michael Wolf,<sup>§</sup> Mark E. Nielsen,<sup>‡</sup> Peter R. Girguis,<sup>‡</sup> and Clare E. Reimers<sup>†,\*</sup>

<sup>†</sup>College of Oceanic & Atmospheric Sciences, Hatfield Marine Science Center, Oregon State University, Newport, Oregon 97365, United States

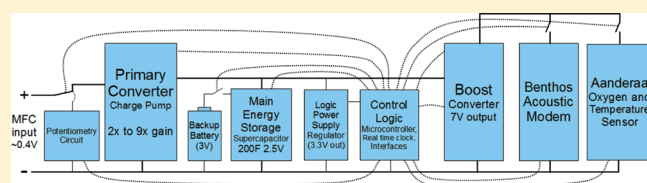
<sup>‡</sup>Biological Laboratories, Harvard University, 16 Divinity Avenue, Cambridge, Massachusetts 02138, United States

<sup>§</sup>Teledyne Benthos, Inc., 49 Edgerton Dr., North Falmouth, Massachusetts 02556-2826, United States

 Supporting Information

**ABSTRACT:** Supported by the natural potential difference between anoxic sediment and oxic seawater, benthic microbial fuel cells (BMFCs) promise to be ideal power sources for certain low-power marine sensors and communication devices. In this study a chambered BMFC with a 0.25 m<sup>2</sup> footprint was used to power an acoustic modem interfaced with an oceanographic sensor that measures dissolved oxygen and temperature.

The experiment was conducted in Yaquina Bay, Oregon over 50 days. Several improvements were made in the BMFC design and power management system based on lessons learned from earlier prototypes. The energy was harvested by a dynamic gain charge pump circuit that maintains a desired point on the BMFC's power curve and stores the energy in a 200 F supercapacitor. The system also used an ultralow power microcontroller and quartz clock to read the oxygen/temperature sensor hourly, store data with a time stamp, and perform daily polarizations. Data records were transmitted to the surface by the acoustic modem every 1–5 days after receiving an acoustic prompt from a surface hydrophone. After jump-starting energy production with supplemental macroalgae placed in the BMFC's anode chamber, the average power density of the BMFC adjusted to 44 mW/m<sup>2</sup> of seafloor area which is better than past demonstrations at this site. The highest power density was 158 mW/m<sup>2</sup>, and the useful energy produced and stored was  $\geq 1.7$  times the energy required to operate the system.



## INTRODUCTION

Microbial fuel cells (MFCs) have appeared in the fuel cell family only within recent decades,<sup>1–3</sup> although their bioelectrochemical activities were first described at the beginning of the 20th century by Potter.<sup>4</sup> Compared to many types of pure chemical fuel cells, such as the hydrogen/oxygen proton exchange membrane fuel cell, the power density generated from MFCs is small.<sup>2</sup> However, advantages including low operating temperature, simple construction, viability in extreme environments, and wide and cheap fuel resources associated with MFCs inspire the long-lasting academic and industrial interest in this technology.

To date, significant progress has been made in using mixed and isolated bacterial strains including *Geobacter* and *Shewanella* as effective biocatalysts within MFCs for harvesting renewable electrical power. Combined wastewater treatment and electricity production is being actively investigated. A wide range of organic substrates, ranging from simple acetate and glucose to complex algal and cellulosic biomass have been successfully demonstrated as fuels.<sup>5–8</sup> These studies have sufficiently identified the promising value of the MFC process, however, perhaps the most practical application of MFCs is to serve as long-term power sources in remote environments such as at the seafloor.

The first functional prototypes of *benthic* microbial fuel cells (BMFCs) were created about 10 years ago, inspired by the experiments of Reimers and Tender.<sup>9,10</sup> BMFCs are bioelectrochemical devices driven by the naturally generated potential difference between anoxic sediment and oxic seawater.<sup>10–13</sup> The sediment layer separating anode from cathode effectively conserves oxygen diffusing from the overlying water column and eliminates a need for an ion-exchange membrane. Organic detritus within the sediment is the source of electron donors which migrate slowly through the sediments to be oxidized at the anode.

BMFCs are very promising power sources for low power marine sensors. Most oceanographic and surveillance instruments on the seafloor have no cable connection with the surface, so they have to run on batteries. The main drawbacks of batteries are limited calendar lifetime, and high cost of periodic replacement, especially in deep water.

BMFCs have been deployed in a variety of configurations. Some research groups rely on solid graphite (plates or rods)

**Received:** December 30, 2010

**Accepted:** April 27, 2011

**Revised:** April 20, 2011

**Published:** May 05, 2011

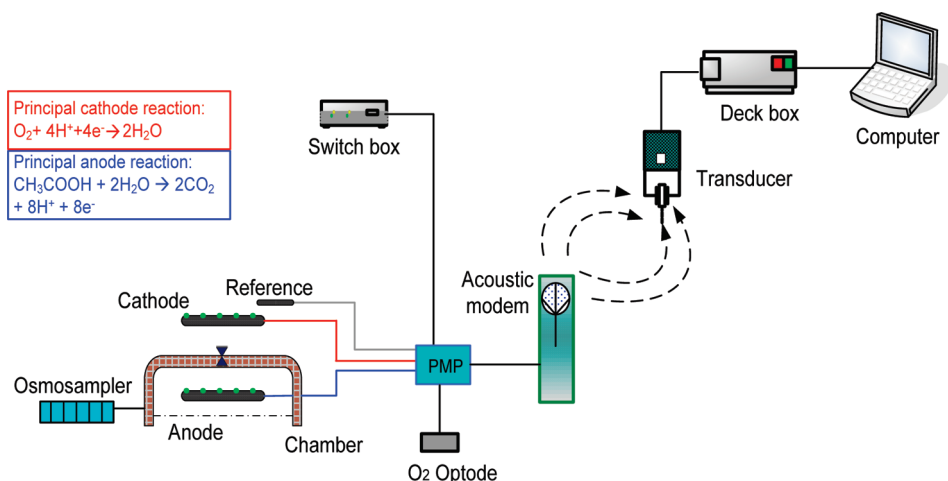


Figure 1. Schematic of overall experimental setup.

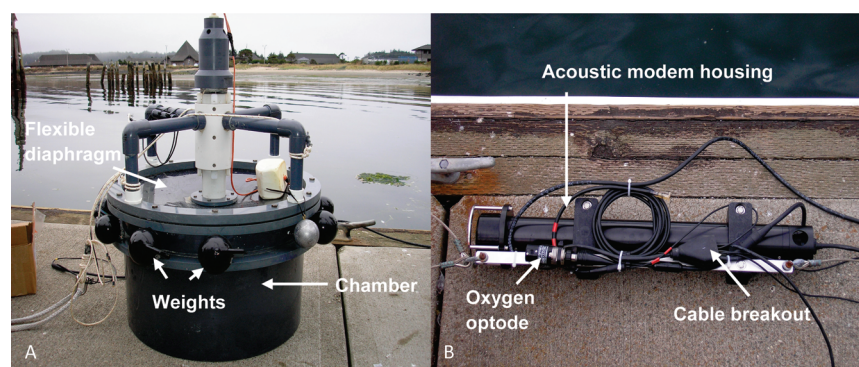


Figure 2. (A) Image of BMFC chamber by Yaquina Bay, Oregon. (B) Image of modem and PMP electronics enclosure with oxygen optode and cabling.

electrodes, burying the anodes within sediments and suspending the cathodes in the overlying seawater on nonconductive frames.<sup>10,14,15</sup> Nielsen et al.<sup>16</sup> developed the chambered BMFC design, in which the anode is contained in a semienclosed chamber that is either pushed into or set atop the sediment.

Although there can be problems with chamber designs such as loss of anoxic conditions around the anode due to a poor seal with the sediments, chambered BMFCs have several unique advantages. These include: easier deployment, the ability to use high surface area electrodes (e.g., carbon-fiber brushes), and the ability to enhance mass transport either mechanically or through natural advection.<sup>16,17</sup> In the past 10 years, the continuous generation of power densities ranging from 1 to 10 mW/m<sup>2</sup> (with areas representing chamber or simple plate electrode footprint) has been demonstrated in a wide variety of marine environments with peak power densities typically 10–30 mW/m<sup>2</sup>.<sup>10,14,16,18</sup> Under unique operational conditions, when a chambered BMFC was deployed at a methane cold seep,<sup>16,17</sup> peak power densities as high as 380 mW/m<sup>2</sup> have been observed.

To date, BMFCs have only just begun to be applied to power a range of environmental sensors and thus to prove themselves as a viable means of providing long-term, uninterrupted power for submarine devices.<sup>14,18,19</sup> In this context, the ability to collect and retrieve undersea data without the use of wired infrastructure is of paramount importance. Therefore, the objective of this study was

to demonstrate the effectiveness of a BMFC as a power source for both a seawater oxygen sensor system and an acoustic modem able to route data from the sensor. We also introduce a new power management platform (PMP) that provides dynamic power conversion and energy storage, and that can schedule sensor readings and communications events while drawing very low quiescent power.

## EXPERIMENTAL SECTION

**BMFC Powered Acoustic Modem, Power Management and Sensor System.** The BMFC was deployed on September 14, 2010 near the ship dock of Oregon State University in Yaquina Bay, Newport, Oregon, at about 7 m water depth (Latitude: 44° 37.5' N, Longitude: 124° 2.5' W). One day later it was connected by underwater pluggable connectors and cables to the acoustic modem and sensor. A schematic of the overall system is shown in Figure 1 and key components are pictured in Figure 2. The electric energy harvested from BMFC was stored in a 200 F supercapacitor (Cooper-Bussman) after charge pump conversion to a higher voltage (variable from 2 to 9 times) by the custom-designed PMP which was enclosed within the acoustic modem housing. The stored energy was utilized to power (1) the oxygen optode (Aanderaa model 4835) for oxygen and temperature measurements, (2) the acoustic modem (Teledyne-Benthos Compact Modem) for data storage and acoustic data transmission, and (3) the PMP.

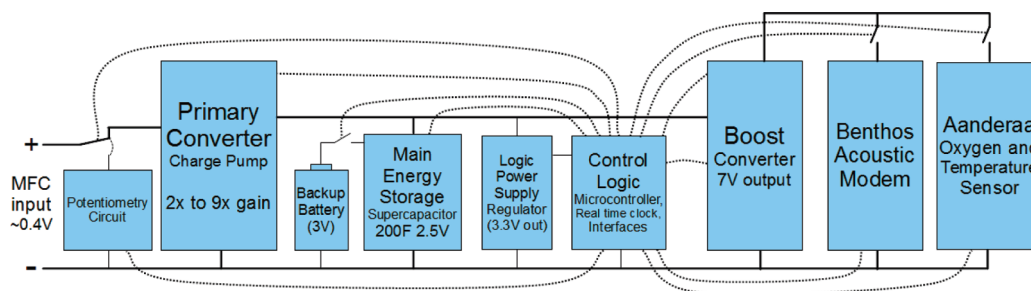


**Figure 3.** Schematic of the power management platform. This system was developed at Trophos Energy (Somerville, MA). A more advanced version is available from Teledyne-Benthos (North Falmouth, MA).

The PMP (Figure 3) included a second-stage boost converter, a circuit to do potential sweeps by generating a variable resistance load across the BMFC, a microcontroller (Texas Instruments MSP430) with real time clock (10 ppm 32768 Hz crystal), and a backup “D-cell” battery pack. The use of the microcontroller was a new development and served to manage energy harvesting, schedule events like sensor readings and potential sweeps, and activate the acoustic modem for communications with the surface. The boost converter was tailored to meet the voltage requirements of both the oxygen optode (5 V minimum) and acoustic modem (7 V minimum). The battery backup pulsed charge into the 200 F storage cap only when the BMFC could not maintain the supercapacitor voltage above 2.0 V. When the capacitor voltage rose to its maximum level of 2.49 V, the BMFC was “released” by the PMP and allowed to rest with only a trickle of current being extracted.

Whole cell voltage (WCV, i.e., the voltage difference between cathode and anode), real-time temperature and dissolved oxygen readings, the voltage of the supercapacitor, and any usage of the back-up battery (as number of pulses) were recorded on an hourly basis. A potential sweep was automatically performed by the PMP every day between 22:00 and 23:00 to capture the I–V characteristics of the BMFC. The resistances applied were  $\infty$  (open circuit) for 28 min, followed by 102, 77, 51, 36, 26, 16, 11, and 6 ohm each for 4 min. WCV and anode potential (vs Ag/AgCl) were recorded at the end of each interval, and energy transfer to the supercapacitor was interrupted during the potential sweep, causing the system to rely entirely on stored power for one hour per day. Up to 8 days of data were stored in a circular buffer within the modem. These data were transmitted after receiving an acoustic command from the surface and recovered to a computer (Figure 1). For convenience, an external switch (switch box) was used to prompt the PMP to activate the modem to listen for the acoustic command. Alternatively, the system could have been programmed to periodically listen for this command from the surface.

**Benthic Microbial Fuel cell.** As shown in Figure 2a, the anode chamber of the BMFC was similar to earlier designs,<sup>16,17,20</sup> with the notable exception of a flexible diaphragm instead of a rigid chamber lid. The diaphragm was made of 0.32 cm thick polyether urethane sheeting underlain by 0.025 cm thick Mylar sheeting. Flexibility of the diaphragm was designed to allow a small degree of pumping of pore fluids from the sediment up into the chamber and out a one-way valve (part no. 45275k33, McMaster-Carr, Elmhurst IL) driven by changes in surface wave or tidal pressure.<sup>21,22</sup> Such pumping is desired to reduce mass transport limitations at the anode.<sup>23–25</sup> The rest of the chamber consisted of a PVC cylinder (footprint of 0.25 m<sup>2</sup>) with an internal

diameter = 0.56 m and height = 0.38 m (fabricated by Accelerate Inc., Upton MA). Both anode and cathode electrodes were assembled using twisted titanium wire and carbon fiber brushes (Kongsberg Maritime AS, Norway and Mill-Rose Industrial, Mentor OH). The anode brush was 4 m long and coiled inside the top 0.1 m section of the chamber. The cathode was 2 m long and suspended along a line, between an anchor and float, outside of the chamber. The cathode and anode chamber were set ~0.5 m apart. Resistances measured from carbon fibers over the length of electrode and connecting cable, prior to deployment, were 1.4 ohm and 1.1 ohm for anode and cathode, respectively.

A key improvement to the chambered BMFC was the addition of a 6.3 mm mesh-size, polyester-woven net across the midsection of the cylindrical anode chamber. The net was designed to minimize degradation in performance due to bioturbation (burrowing organisms that might pump oxygenated water into the chamber). Ten weights (2–3 kg) were affixed around the chamber cap for stabilization (Figure 2).

Three steps were taken at the start of the BMFC deployment to speed up the initiation of bioelectrical energy production. First, the cathode was preconditioned by submerging into a seawater tank for two weeks so that it held a potential of +330 mV vs Ag/AgCl before the deployment. Second, a potential of ~420 mV ( $\pm$  about 50 mV) was applied by the charge pump between the cathode and anode which poised the anode near 0 mV vs Ag/AgCl. Previous studies have suggested that elevating anode potentials will stimulate electrogenic biofilm growth.<sup>26–28</sup> Third, to jump-start BMFC reactions over the short-term, 562 g wet weight of macroalgae was intentionally placed into the chamber. Using total energies produced from wet weights of marine plankton in previous batch experiments as a guide (0.03–0.08 kJ/g),<sup>29</sup> this quantity of macroalgae was expected to fuel the production of between 17 and 45 kJ of electrical energy.

Lastly, to obtain a continuous record of chemical and microbiological properties of the seawater surrounding the anode, an osmotic pumping system<sup>30,31</sup> was installed and connected to the BMFC chamber for automatically and slowly pulling very small volumes of seawater (~1 mL/day) from the chamber. The osmosampling system is simple, reliable and has no energy requirement. Analyses of these samples will be the subject of later research and reporting.

## RESULTS AND DISCUSSION

**Effect of Cell Poising, Cathode Conditioning and Macroalgae.** Figure 4 shows the BMFC was able to provide the energy needs of the acoustic modem and sensor system by the fifth day of deployment. Prior to day 5, energy was drawn from the backup



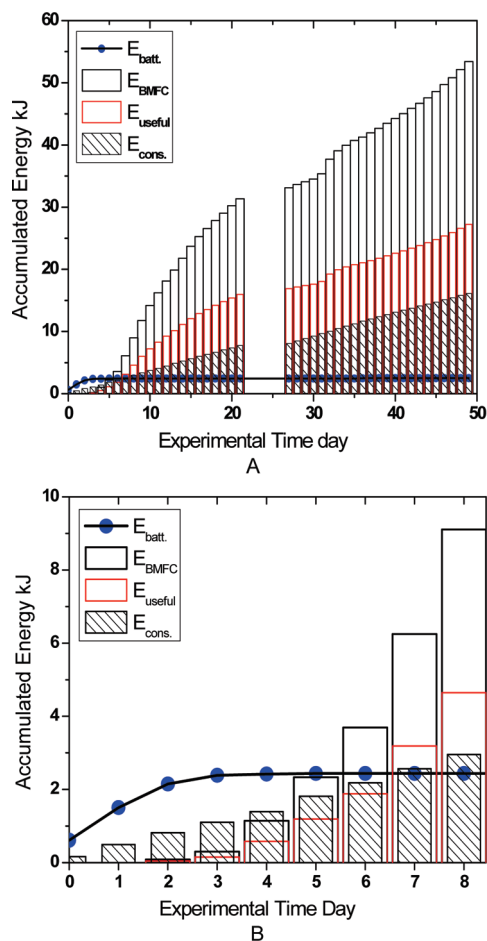


**Figure 4.** (A) Accumulated 50-day (day 0–day 49) and (B) accumulated first 8-day energy budget of the BMFC-acoustic modem and sensor system.  $E_{\text{batt}}$  is the accumulated energy drawn from the backup battery;  $E_{\text{BMFC}}$  is the accumulated energy produced by the BMFC;  $E_{\text{useful}}$  is defined as the available energy after the two stages of energy conversion to higher voltage;  $E_{\text{cons}}$  is an estimate of the cumulative energy consumed by the power management board, acoustic modem, and sensor. A 5-day data gap (day 22–26; 7 October 2010 to 11 October 2010) was caused by a PMP reset which erased this part of the data record before it was recovered acoustically.

battery to maintain the potential of the main energy storage supercapacitor while the primary converter charge pump drew upon this energy to poise the whole cell. The daily potential sweep was also part of the cell conditioning regime, drawing the cell from open circuit down to a very heavy load. The sweeps allowed the anode to float to negative potentials (vs Ag/AgCl), and then pulled the anode to positive potentials close to the cathode potential. In earlier studies, the initiation of BMFC power generation has required 2–3 weeks or even longer. The shortened start-up time observed in this study is attributed to the combined effects of the dynamic regime of poisoning electrode potentials, and adding supplemental algae as an initial feedstock. Past research suggests that positive anode potentials encourage enrichments of electrogenic bacteria within anode biofilms.<sup>32–34</sup> Furthermore, Wang et al.<sup>33</sup> reported that the application of a +200 mV vs Ag/AgCl poisoning potential to the anode of a MFC reduced the time required to obtain equivalent power output from 59 to 25 days. In previous batch experiments

with fresh plankton the initiation of energy production was also rapid.<sup>29</sup> Cathode preconditioning was not fully effective as will be shown in discussion of polarization results below.

**Energy Budget.** A 50-day cumulative energy budget calculated for the BMFC-powered Acoustic Modem/Sensor package is shown in Figure 4. The budget components are  $E_{\text{BMFC}}$ , the energy harvested by the BMFC estimated from daily polarization curves and hourly recorded whole cell potentials;  $E_{\text{batt}}$ , the energy supplied by the backup battery when the voltage of the supercapacitor was lower than a minimum of 2.0 V (this was usually zero);  $E_{\text{useful}}$ , the energy available for the sensor and modem system; and  $E_{\text{cons}}$ , the energy consumed. The energy budget was determined by computing the above components daily and summing them cumulatively over time.

The amount of useful energy from the BMFC ( $E_{\text{useful}}$ ) is defined as

$$E_{\text{useful}} = \eta_1 \eta_2 E_{\text{BMFC}} \quad (1)$$

where  $\eta_1$  is the efficiency of the primary converter; and  $\eta_2$  is the efficiency of the boost converter (Figure 3). In practice, these efficiency values are variable and will change with operating conditions. For simplicity, we assumed  $\eta_1 = 0.85$  and  $\eta_2 = 0.6$  which are conservative values as verified by laboratory testing of a matrix of input and output power levels.  $E_{\text{cons}}$  was calculated as:

$$E_{\text{cons}} = E_{\text{mq}} + E_{\text{bq}} + E_{\text{trans}} + E_{\text{optode}} \quad (2)$$

where,  $E_{\text{mq}}$  is the energy needed to maintain the acoustic modem in a quiescent state (3 mW);  $E_{\text{bq}}$  is the minimum energy required to maintain the duties of the power management platform including the internal clock (45  $\mu\text{W}$ );  $E_{\text{trans}}$  is the energy consumed when the stored data was remotely transmitted from the deployment site to shore by acoustic modem; and  $E_{\text{optode}}$  is the energy consumed by the oxygen optode for hourly oxygen and temperature readings (each = 250 mW  $\times$  3 s = 0.75 J). During this experiment, daily values of  $E_{\text{trans}}$  were dependent on how often data files were retrieved and thus the size of the recovered data file. One day's data equaled 1.1KB and 40 J were consumed per KB. Three detailed examples of daily energy budget calculations are presented as Supporting Information.

Figure 4 illustrates that the accumulated electrical energy produced from the BMFC was enough to sustain the overall system. The day 22–26 record of energy production and consumption was lost due to an unexpected reset of the PMP (see discussion below) that erased the interim data file and so this period is omitted from the budget analysis. A total of 53.5 kJ electrical energy was documented as generated by the BMFC, and this total was 3.3 times the amount of electric energy required (16.1 kJ) to keep the overall system running. However, not all the electrical energy could be utilized or stored as what we have called “useful energy”. The calculated useful energy,  $E_{\text{useful}}$ , was 27.3 kJ or 1.7 times the energy required. The difference between  $E_{\text{BMFC}}$  and  $E_{\text{useful}}$  is due to the presumed costs of power conversion from the low voltage ( $\sim 0.4$  V) of the BMFC to the different voltage needs of the oxygen optode and the acoustic modem.

As described earlier, the measurement frequency of the oxygen optode was programmed as once per hour and energy was required each time the optode was turned on to collect data. The extra energy produced during this experiment should have been sufficient to support data readings at a rate of once every 12 min.

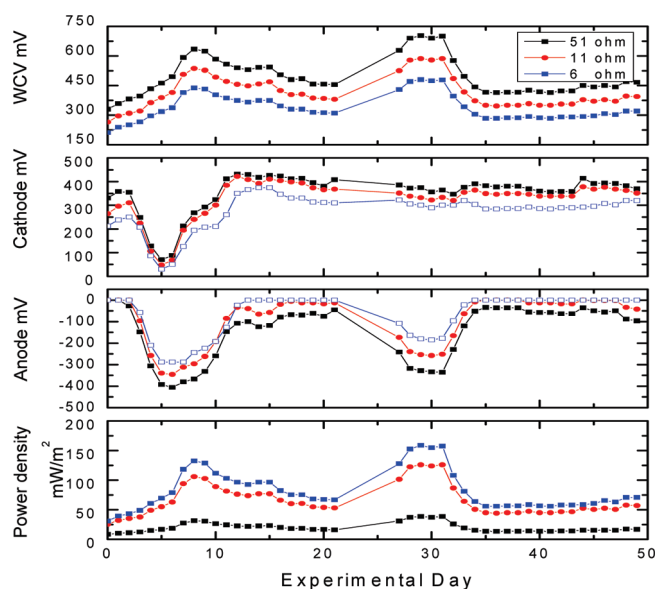


**Figure 5.** Evolution of whole cell potential (WCV), cathode and anode potential vs Ag/AgCl, and power densities (vs chamber footprint) at variable resistances. Positive values of anode potential (observed primarily at 6 ohm) appear clamped at 0 V due to limitations of the analog to digital converter.

This calculation takes into account sensor power requirements and additional energy needed to transmit larger data files.

In future designs, we anticipate higher sampling rates may be supported by improving the efficiency of the PMP voltage-boost technique. We have discovered a source of an intermittent power leakage that was associated with the way the PMP was sending power to the modem. Although this problem has since been corrected, it probably added to  $E_{\text{cons}}$  and thus put a higher demand on the BMFC than we have calculated. The problematic PMP reset has been diagnosed as due to a high rush of current when the oxygen optode was switched on. This has also been corrected. In addition, with the PMP board design used in this study, the supercapacitor had a limited storage capacity which was sufficient as a buffer but not ideal for energy storage. Most of the extra energy was not saved due to the constraint of storage. This will be an important issue to be addressed in later PMP board designs perhaps by incorporating Lithium-ion cells as larger capacity energy storage components.

**Polarization Performance of BMFC.** Daily polarization measurements document how the power production characteristics of the BMFC changed over time. These measurements were also used with hourly WCV readings to estimate the  $E_{\text{BMFC}}$  (see Supporting Information). Figure 5 shows the evolution of power densities, whole cell potentials (WCV), anode potentials and cathode potentials at external resistances of 6, 11, and 51 ohms. The data for the first 5 days reflects the period when the open circuit cell potential was not yet up to  $\sim 420$  mV causing the charge pump to draw from the backup battery to poise the cell. Data records were also lost for the period between days 22 and 26 as discussed above. Over the experimental period of 50 days, the highest power densities determined were  $\sim 158$  mW/m<sup>2</sup> during the period of day 28–31.

Consistent with a combination of Ohm's and Joule's Law ( $P = E_{\text{cell}}^2/R_{\text{external}}$ ), changes in electrode potentials follow changes of power densities. For example from day 31 to 35 at

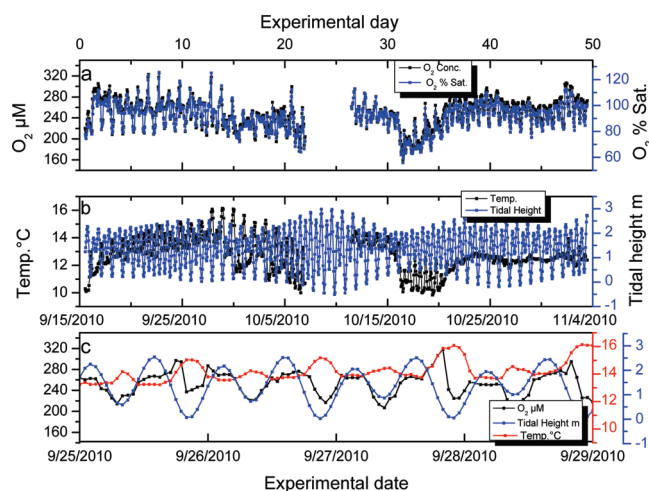


**Figure 6.** (a) Hourly oxygen concentration and % saturation and (b) temperature measured in Yaquina Bay, over 50 days. In (b) independent tidal height measurements from NOAA station no. 9435380 (<http://tidesandcurrents.noaa.gov/>) are also reported. The oxygen concentrations were calculated from sensor readings and hourly salinity measurements from an independent sensor maintained by the EPA Western Ecology Division. (c). Short-term correspondence of changes in temperature, oxygen concentration and tidal height.

51 ohm, when the power density fell from 38 to 13 mW/m<sup>2</sup>, the anode potential changed from  $-336$  to  $-34$  mV, however, the cathode potential was quite independent of the variation of power density. No significant change of the cathode potential was observed after an initial equilibration period that took a surprising 11 days even though the cathode had been preconditioned in raw seawater. From Figure 5, we conclude that the magnitude of the anode overpotential was by day 35 much greater than the cathode overpotential. This finding is consistent with power limitation arising from the mass transport of reductants to the anode and/or rates of anode reactions. Factors that were likely to have caused variations in anode processes include (1) the differential degradation of the supplemental algae added to the BMFC, (2) variations in load history stemming from changes in  $E_{\text{cons}}$  as well as the energy leakages and system reset noted above, and (3) the strength of tidal pumping. The highest tidal change through the 50 day experimental period, occurred prior to and during the days of peak power from day 27 to 31 (between  $-0.5$  and  $2.9$  m; Figure 6). According to our energy budget and past batch experiments, we expect most (if not all) of the energy available from the macroalgae was consumed by day 35. This implies the nearly steady power density (averaging 44 mW/m<sup>2</sup>) observed over the final 15 days of this experiment was supported by endogenous electron donors in the sediment. In addition, if this power level was sustained over the long-term, the system should have run indefinitely (see Supporting Information).

**Oxygen Optode Data Record.** As proof of the practical application of a BMFC, Figure 6 presents the nearly real-time temperature and dissolved oxygen data delivered by the oxygen optode, PMP and acoustic modem. The oxygen optode used in this experiment was completely powered by the electrical energy from the BMFC which was managed by the power management platform, except during days 0–5 of the experiment (Figure 4) when the BMFC was coming up to power.

Figure 6c shows details of how the recovered temperature and dissolved oxygen near the seabed were influenced by the mixed

**Table 1.** Pearson Correlation Coefficients (PMCC) of O<sub>2</sub> Concentration, Water Temperature, Tidal Height, and O<sub>2</sub> Saturation %

	O <sub>2</sub> concentration	temperature	tidal height	O <sub>2</sub> saturation %
O <sub>2</sub> concentration	1	0.25	0.30	0.98
temperature	0.25	1	−0.36	0.41
tidal height	0.30	−0.36	1	0.23
O <sub>2</sub> saturation %	0.98	0.41	0.23	1

tides and circulation patterns in the estuary. We observed that dissolved oxygen increased and temperature decreased with the strength of the incoming tide, and the dissolved oxygen decreased and temperature increased with the strength of the outgoing tide. (Table 1 gives Pearson correlation coefficients between these parameters over the entire data set showing medium correlation strengths between most variables.) These patterns are typical characteristics of a Northeast Pacific estuary during autumn conditions when the river discharge is just beginning to ramp up.<sup>35,36</sup> Nearly air-saturated to supersaturated, colder and saltier water is mixed into the bay from the ocean; whereas, undersaturated, warmer and fresher water is supplied by the river and upper estuary each time the tide recedes.

**Future Directions.** The present study suggests several paths for future research and development toward improving BMFCs as an effective energy source for seafloor instrumentation. These are:

- Research into the effects of dynamic cell operation: The BMFC started up quickly and powerfully using a dynamic regime of electrode poisoning and daily potential sweeps. There is almost no literature on the effects of dynamic regimes on continuing operation of microbial fuel cells. A factorial experiment to separate the individual and combinatory effects of various elements of the regime would be fruitful.
- Research into the effects of preloading the benthic chamber with various amounts, types, and release regimes of biofuel: The present experiment used a single addition of algae. Only one study<sup>20</sup> has examined repeated supplementation and its effects on sustained power generation.
- Enhancement of the instrumentation of the Power Management Platform for study of the BMFC as a power source: Future systems should be able read both positive and negative electrode voltages versus the reference electrode, and to sense the current drawn while harvesting energy instead of only when doing a potential sweep. Enhancing the data storage for better temporal resolution and backup of data would also be useful.
- Enhancement of the voltage boost efficiency and energy storage capacity of the PMP, and further integration of bidirectional low-power acoustic communications techniques: The present system was not optimized especially in the efficiency of the boost converter. We also did not go as far as to develop capability to control factors such as the sampling frequency of the sensor by acoustic command.
- Identification, development, and testing of other sensors, to record data such as ocean salinity, pressure, turbidity, pH, and water current velocity: These integrations should inspire greater development of low-power sensors and sensor network devices.

## ■ ASSOCIATED CONTENT

**S Supporting Information.** Additional information concerning eqs 1 and 2 and a table of energy budget numbers from three separate days. This material is available free of charge via the Internet at <http://pubs.acs.org>.

## ■ AUTHOR INFORMATION

### Corresponding Author

\*E-mail: [creimers@coas.oregonstate.edu](mailto:creimers@coas.oregonstate.edu).

## ■ ACKNOWLEDGMENT

We greatly thank Kristina McCann-Grosvenor, Rhea Sanders, and Daryl Swensen (Oregon State University) for their diving support. Dale Green and Michael Chiu were instrumental in organizing this collaborative effort. This work was funded by the Office of Naval Research under Grant No. N000140910199 to C.R.

## ■ REFERENCES

- (1) Girguis, P. R.; Nielsen, M. E.; Figueroa, I. Harnessing energy from marine productivity using bioelectrochemical systems. *Curr. Opin. Biotechnol.* **2010**, *21* (3), 252–258.
- (2) Bullen, R. A.; Arnot, T. C.; Lakeman, J. B.; Walsh, F. C. Biofuel cells and their development. *Biosens. Bioelectron.* **2006**, *21* (11), 2015–2045.
- (3) Franks, A. E.; Nevin, K. P. Microbial fuel cells, a current review. *Energies* **2010**, *3* (5), 899–919.
- (4) Potter, C. M. Electrical effects accompanying the decomposition of organic compounds. *Proc. R. Soc. London* **1911**, *Series B*, 260–276.
- (5) Velasquez-Orta, S. B.; Curtis, T. P.; Logan, B. E. Energy from algae using microbial fuel cells. *Biotechnol. Bioeng.* **2009**, *103* (6), 1068–1076.
- (6) Liu, H.; Cheng, S. A.; Logan, B. E. Production of electricity from acetate or butyrate using a single-chamber microbial fuel cell. *Environ. Sci. Technol.* **2005**, *39* (2), 658–662.
- (7) Bond, D. R.; Lovley, D. R. Electricity production by *Geobacter sulfurreducens* attached to electrodes. *Appl. Environ. Microbiol.* **2003**, *69* (3), 1548–1555.
- (8) Ren, Z.; Steinberg, L. M.; Regan, J. M. Electricity production and microbial biofilm characterization in cellulose-fed microbial fuel cells. *Water Sci. Technol.* **2008**, *58* (3), 617–622.
- (9) Reimers, C. E.; Tender, L. M.; Fertig, S.; Wang, W. Harvesting energy from the marine sediment-water interface. *Environ. Sci. Technol.* **2001**, *35* (1), 192–195.
- (10) Tender, L. M.; Reimers, C. E.; Stecher, H. A.; Holmes, D. E.; Bond, D. R.; Lowy, D. A.; Pilobello, K.; Fertig, S. J.; Lovley, D. R. Harnessing microbially generated power on the seafloor. *Nat. Biotechnol.* **2002**, *20* (8), 821–825.
- (11) Lovley, D. R. Bug juice: harvesting electricity with microorganisms. *Nat. Rev. Microbiol.* **2006**, *4* (7), 497–508.
- (12) Bond, D. R.; Holmes, D. E.; Tender, L. M.; Lovley, D. R. Electrode-reducing microorganisms that harvest energy from marine sediments. *Science* **2002**, *295* (5554), 483–485.
- (13) Reimers, C. E.; Girguis, P. R.; Stecher, H. A., III; Tender, L. M.; Ryckelynck, N.; Whaling, P. Microbial fuel cell energy from an ocean cold seep. *Geobiology* **2006**, *4* (2), 123–136.
- (14) Tender, L. M.; Gray, S. A.; Groveman, E.; Lowy, D. A.; Kauffman, P.; Melhado, J.; Tyce, R. C.; Flynn, D.; Petrecca, R.; Dobarro, J. The first demonstration of a microbial fuel cell as a viable power supply: Powering a meteorological buoy. *J. Power Sources* **2008**, *179* (2), 571–575.
- (15) Dewan, A.; Donovan, C.; Heo, D.; Beyenal, H. Evaluating the performance of microbial fuel cells powering electronic devices. *J. Power Sources* **2010**, *195* (1), 90–96.



- (16) Nielsen, M. E.; Reimers, C. E.; Stecher, H. A. Enhanced power from chambered benthic microbial fuel cells. *Environ. Sci. Technol.* **2007**, *41* (22), 7895–7900.
- (17) Nielsen, M. E.; Reimers, C. E.; White, H. K.; Sharma, S.; Girguis, P. R. Sustainable energy from deep ocean cold seeps. *Energy Environ. Sci.* **2008**, *1* (5), 584–593.
- (18) Wotawa-Bergen, A. Q.; Chadwick, D. B.; Richter, K. E.; Tender, L. M.; Reimers, C. E.; Gong, Y. Operational testing of sediment-based microbial fuel cells in the San Diego Bay. In *2010 IEEE Oceans Conference Proceedings*, 2010; pp 1–6.
- (19) Donovan, C.; Dewar, A.; Heo, D.; Beyenal, H. Batteryless, wireless sensor powered by a sediment microbial fuel cell. *Environ. Sci. Technol.* **2008**, *42* (22), 8591–8596.
- (20) Nielsen, M. E.; Wu, D. M.; Girguis, P. R.; Reimers, C. E. Influence of substrate on electron transfer mechanisms in chambered benthic microbial fuel cells. *Environ. Sci. Technol.* **2009**, *43* (22), 8671–8677.
- (21) Malan, D. E.; McLachlan, A. In situ benthic oxygen fluxes in a nearshore coastal marine system: a new approach to quantify the effect of wave action. *Mar. Ecol.: Prog. Ser.* **1991**, *73*, 69–81.
- (22) Webb, J. E.; Theodor, J. L. Wave-induced circulation in submerged sands. *J. Mar. Biol. Assoc. U.K.* **1972**, *52* (2), 903–914.
- (23) Mathuriya, A. S.; Sharma, V. N. Bioelectricity production from various wastewaters through microbial fuel cell technology. *J. Biochem. Technol.* **2009**, *2* (1), 133–137.
- (24) Rabaey, K.; Clauwaert, P.; Aelterman, P.; Verstraete, W. Tubular microbial fuel cells for efficient electricity generation. *Environ. Sci. Technol.* **2005**, *39* (20), 8077–8082.
- (25) Cheng, S.; Liu, H.; Logan, B. E. Increased power generation in a continuous flow MFC with advective flow through the porous anode and reduced electrode spacing. *Environ. Sci. Technol.* **2006**, *40* (7), 2426–2432.
- (26) Finkelstein, D. A.; Tender, L. M.; Zeikus, J. G. Effect of electrode potential on electrode-reducing microbiota. *Environ. Sci. Technol.* **2006**, *40* (22), 6990–6995.
- (27) Aelterman, P.; Freguia, S.; Keller, J.; Verstraete, W.; Rabaey, K. The anode potential regulates bacterial activity in microbial fuel cells. *Appl. Microbiol. Biotechnol.* **2008**, *78* (3), 409–418.
- (28) Torres, C. I.; Krajmalnik-Brown, R.; Parameswaran, P.; Marcus, A. K.; Wanger, G.; Gorby, Y. A.; Rittmann, B. E. Selecting anode-respiring bacteria based on anode potential: Phylogenetic, electrochemical, and microscopic characterization. *Environ. Sci. Technol.* **2009**, *43* (24), 9519–9524.
- (29) Reimers, C. E.; Stecher, H. A., III; Westall, J. C.; Alleau, Y.; Howell, K. A.; Soule, L.; White, H. K.; Girguis, P. R. Substrate degradation kinetics, microbial diversity, and current efficiency of microbial fuel cells supplied with marine plankton. *Appl. Environ. Microbiol.* **2007**, *73* (21), 7029–7040.
- (30) Jannasch, H. W.; Wheat, G. C.; Plant, J. N.; Kastner, M.; Stakes, D. S. Continuous chemical monitoring with osmotically pumped water samplers: OsmoSampler design and application. *Limnol. Oceanogr.: Methods* **2004**, *2*, 102–113.
- (31) Jannasch, H. W.; Johnson, K. S.; Sakamoto, C. M. Submersible, osmotically pumped analyzers for continuous determination of nitrate in-situ. *Anal. Chem.* **1994**, *66* (20), 3352–3361.
- (32) Ryckelynck, N.; Stecher, H. A.; Reimers, C. E. Understanding the anodic mechanism of a seafloor fuel cell: Interactions between geochemistry and microbial activity. *Biogeochemistry* **2005**, *76* (1), 113–139.
- (33) Wang, X.; Feng, Y. J.; Ren, N. Q.; Wang, H. M.; Lee, H.; Li, N.; Zhao, Q. L. Accelerated start-up of two-chambered microbial fuel cells: Effect of anodic positive poised potential. *Electrochim. Acta* **2009**, *54* (3), 1109–1114.
- (34) Kim, B. H.; Kim, H. J.; Hyun, M. S.; Park, D. H. Direct electrode reaction of Fe(III)-reducing bacterium, *Shewanella putrefaciens*. *J. Microbiol. Biotechnol.* **1999**, *9* (2), 127–131.
- (35) Sigleo, A. C.; Frick, W. E. Seasonal variations in river discharge and nutrient export to a Northeastern Pacific estuary. *Estuarine, Coastal Shelf Sci.* **2007**, *73* (3–4), 368–378.
- (36) Komar, P. D. *Beach Processes and Sedimentation*, 1st ed.; Prentice-Hall, Inc.: Englewood Cliffs, NJ, 1976; pp 134–146.